

David A. Collings · John D. I. Harper · Kevin C. Vaughn

## The association of peroxisomes with the developing cell plate in dividing onion root cells depends on actin microfilaments and myosin

Received: 5 April 2003 / Accepted: 23 June 2003 / Published online: 21 August 2003  
© Springer-Verlag 2003

**Abstract** We have investigated changes in the distribution of peroxisomes through the cell cycle in onion (*Allium cepa* L.) root meristem cells with immunofluorescence and electron microscopy, and in leek (*Allium porrum* L.) epidermal cells with immunofluorescence and peroxisomal-targeted green fluorescent protein. During interphase and mitosis, peroxisomes distribute randomly throughout the cytoplasm, but beginning late in anaphase, they accumulate at the division plane. Initially, peroxisomes occur within the microtubule phragmoplast in two zones on either side of the developing cell plate. However, as the phragmoplast expands outwards to form an annulus, peroxisomes redistribute into a ring immediately inside the location of the microtubules. Peroxisome aggregation depends on actin microfilaments and myosin. Peroxisomes first accumulate in the division plane prior to the formation of the microtubule phragmoplast, and throughout cytokinesis, always colocalise with microfilaments. Microfilament-disrupting drugs (cytochalasin and latrunculin), and a putative inhibitor of myosin (2,3-butanedione monoxime), inhibit aggregation. We propose that aggregated peroxisomes function in the formation of the cell plate, either by regulating hydrogen peroxide production within the developing cell plate, or by their involvement in recycling of excess membranes from secretory vesicles via the  $\beta$ -oxidation pathway. Differences in aggregation, a phenomenon which occurs in onion, some other monocots and to a lesser extent in tobacco BY-2 suspension cells, but which is not obvious in the roots of *Arabidopsis thaliana* (L.) Heynh., may reflect differences within the primary cell walls of these plants.

cling of excess membranes from secretory vesicles via the  $\beta$ -oxidation pathway. Differences in aggregation, a phenomenon which occurs in onion, some other monocots and to a lesser extent in tobacco BY-2 suspension cells, but which is not obvious in the roots of *Arabidopsis thaliana* (L.) Heynh., may reflect differences within the primary cell walls of these plants.

**Keywords** Actin microfilaments · *Allium* · Microtubule · Cell plate · Peroxisome · Phragmoplast

**Abbreviations** *BDM*: 2,3-butanedione monoxime · *DAPI*: 4',6-diamidino-2-phenylindole · *ER*: endoplasmic reticulum · *GFP*: green fluorescent protein

### Introduction

Mitosis involves the equal partitioning of nuclear material into two daughter cells. The role of microtubules in chromosome segregation, and their organisation through cell division into the division-specific arrays of the preprophase band, mitotic spindle and phragmoplast have been extensively characterised in many different plants (Otegui and Staehelin 2000). Actin microfilament organisation during cell division has also been described, with the division-specific arrays of the microfilament preprophase band and phragmoplast forming in addition to the retention of extensive arrays throughout the cytoplasm (Schmit 2000).

Cell division, however, involves more than just the nuclear material during mitosis. During cytokinesis, each daughter cell must receive a full complement of cytoplasmic components, notably self-replicating organelles that do not arise de novo. In plants, this cytoplasmic partitioning is not understood as thoroughly as nuclear division. Some organelles partition because of their random distribution through the cytoplasm, for example plant mitochondria (Nebenführ et al. 2000), but a random distribution would suggest that

---

D. A. Collings (✉)  
Plant Cell Biology Group, Research School of Biological Sciences,  
Australian National University, GPO Box 475, Canberra,  
ACT 2601, Australia  
E-mail: collings@rsbs.anu.edu.au  
Fax: +61-2-61254331

D. A. Collings  
School of Biological Sciences, Sydney University,  
NSW 2006, Australia

J. D. I. Harper  
Farrer Centre, School of Agriculture, Charles Sturt University,  
Locked Bag 588, Wagga Wagga, NSW 2678, Australia

K. C. Vaughn  
Southern Weed Science Research Unit, USDA-ARS,  
PO Box 350, Stoneville, MS 38776, USA

such organelles do not themselves play a role in the division process. As cytokinesis involves the deposition of cell wall material during the formation and rapid outward expansion of the cell plate, certain organelles are required for division. The non-random distributions of the endoplasmic reticulum (ER) and Golgi apparatus during cytokinesis (Nebenführ et al. 2000) correspond to their functions, as the formation of the new cell wall requires the fusion of ER- and Golgi-derived vesicles within the phragmoplast and cell plate (Samuels et al. 1995). Potential roles for other organelles in the division of plant cells remain unexplored.

Plant peroxisomes are generally small (0.3–1.5 µm diameter) and numerous. They function in the containment and metabolism of hydrogen peroxide, a membrane-permeant and potentially damaging reactive oxygen species that is generated by various oxidases during the oxidation of substrates, and during certain cellular signalling processes (van Breusegem et al. 2001). Plant peroxisomes also function in the β-oxidation of fatty acids, and thus play an important role in the synthesis and turnover of membrane lipids, including during senescence (Gerhardt 1986, 1992). In specialised plant tissues, peroxisomes also catalyse numerous further reactions, including the glyoxylate cycle of oilseeds, and photorespiration in leaves (Mullen et al. 2001; Reumann 2002). Much, however, remains to be learned about the function of peroxisomes in plants. For example, mutations in the *Arabidopsis TED3* gene, which encodes a peroxisomal protein, can suppress mutations in the *DET* gene that encodes an essential nuclear protein that acts as a repressor in photomorphogenesis. The mechanism for this interaction remains poorly understood (Hu et al. 2002).

Our current study of peroxisomal distribution during cell division evolved from a series of experiments that used peroxisomal-targeted green fluorescent protein (GFP) to observe peroxisome motility in the interphase cells of leek epidermis (Collings et al. 2002). These and other studies showed that peroxisomes move rapidly through the cytoplasm of interphase cells, translocated by myosin motors along microfilament bundles (Collings et al. 2002; Jedd and Chua 2002; Mano et al. 2002; Mathur et al. 2002), but they did not report on the localisation of peroxisomes during cell division. However, two early electron-microscopy studies of cell division in the roots of onion (*Allium cepa*; Porter and Machado 1960; Hanzely and Vigil 1975) showed peroxisome-like organelles associated with the cell plate during division, although Porter and Machado (1960), who worked in an era before peroxisomes had been discovered, referred to the as then unknown organelles as phragmosomes. Therefore, we commenced a series of immunolabelling studies using the peroxisomal marker enzyme catalase in onion roots. Significantly, we found that the random distribution of peroxisomes during interphase and mitosis is replaced by a specific, microfilament-dependent placement of peroxisomes in the phragmoplast and cell plate. Our observations suggest

some role for peroxisomes in the construction of the cell plate, possibly in strengthening or hardening the new cell wall, or in the recycling of membranes.

## Materials and methods

### Plant material

Seeds of onion [*Allium cepa* L. either Gladalan Brown (Yates, Sydney, NSW, Australia) or Red Hamburger (Park's Seed, Greenwood, SC, USA)] were germinated on moistened paper in full darkness in sealed petri-dishes at 20 °C and used when the roots were 10–25 mm long, about 4 to 5 days after germination. Seed of *Arabidopsis thaliana* (L.) Heynh. ecotype Columbia was grown on 1.2% agar plates containing Hoagland's media and 3% sucrose at 21 °C, and 5-day-old seedlings used when roots were 20 mm long. Tobacco (*Nicotiana tabacum* L.) BY-2 suspension culture cells were grown under standard conditions (Collings et al. 1998), and used during logarithmic growth. Mature leeks (*Allium porrum* L.) were purchased from a local market.

### Antibodies

Primary antibodies used, and their dilutions for immunofluorescence, were: mouse monoclonal anti-α-tubulin (1/1,000; clone B512; Sigma); rabbit polyclonal anti-cottonseed catalase (1/1,000; provided by Dr. R.N. Trelease, Arizona State University); mouse monoclonal anti-tobacco catalase (1/2; Princeton University Monoclonal Antibody Facility); rabbit polyclonal anti-maize pollen actin (1/200; a gift from Dr. C.J. Staiger, Purdue University); and, mouse monoclonal anti-chicken actin (1/200; clone C4; ICN Biomedicals, Seven Hills, NSW, Australia). Secondary antibodies and dilutions were: fluorescein isothiocyanate (FITC)-conjugated sheep anti-mouse IgG and FITC-conjugated sheep anti-rabbit IgG (1/30 and 1/50; Silenus-Amrad, Boronia, VIC, Australia); Alexa 488-conjugated species-specific goat anti-rabbit IgG, and Alexa 546-conjugated species-specific goat anti-mouse IgG (all 1/500; Molecular Probes, Eugene, OR, USA); Cy-3-conjugated sheep anti-rabbit IgG (1/3,000; Sigma) and Cy-5-conjugated goat anti-mouse IgG (Jackson, West Grove, PA, USA).

### Inhibitor studies

The following inhibitors were stored frozen as stock solutions in dimethyl sulfoxide (DMSO): cytochalasin D, and 2,3-butanedione 2-monoxime (BDM; Sigma; 20 mM and 3 M, respectively); and latrunculin B (ICN; 2 mM). Solutions of caffeine and dichlobenil (2,6-dichlorobenzonitrile; Sigma) were made fresh in distilled water upon use.

Whole onion seedlings (4–5 days old) were exposed to inhibitors for 3 h by placing the root tips (5 mm) in a 500-µl drop of inhibitor solution which had been placed on a Parafilm disc within a covered 30-mm-diameter plastic petri dish. Inhibitors were dissolved in distilled water that contained a final concentration of 1.0% DMSO, which was used to solubilise the various inhibitors in the 100- and 1,000-fold stock solutions. Control experiments showed that this immersion in DMSO and water caused no detectable changes in the cytoskeleton or peroxisomal distribution.

### Immunolabelling of onion root cells

Excised 3- to 5-mm-long root tips were fixed for 60 min in PME buffer (50 mM Pipes pH 7.0 K<sup>+</sup>, 2 mM MgSO<sub>4</sub>, 2 mM EGTA, 0.1% Triton X-100) containing 4% formaldehyde and 2 mM phenylmethylsulfonyl fluoride (PMSF), then washed in PME

(3×10 min). Cell walls were digested (10–13 min) with 1% (w/v) cellulysin Y6 and 0.1% pectolyase Y23 (ICN) in PME containing 1% bovine serum albumin (BSA) and 2 mM PMSF. Root tips were washed in PME (3×10 min), and then squashed between two multiwell slides (ICN) coated with 0.1% polyethyleneimine (Sigma). Samples on slides were kept in liquid throughout the procedure. Cells were extracted with methanol at –20 °C (10 min) then rehydrated in phosphate-buffered saline (PBS; 131 mM NaCl, 5.1 mM Na<sub>2</sub>HPO<sub>4</sub>, 1.56 mM KH<sub>2</sub>PO<sub>4</sub>, pH 7.2) for 5 min before blocking in incubation buffer (PBS containing 1% BSA, 0.05% Tween 20, 50 mM glycine; 15 min). Incubations of primary and secondary antibodies, diluted in incubation buffer, were for either for 1 h at 20 °C or overnight at 4 °C, with antibodies in multiple labelling experiments applied concurrently. Washes with PBS containing 50 mM glycine (3×10 min) were run after each antibody incubation. Cells were stained with 0.1 µg ml<sup>-1</sup> 4',6-diamidino-2-phenylindole (DAPI; Sigma) in PBS (5 min), rinsed briefly in PBS and mounted using Citifluor antifade agent (Alltech, Baukham Hills, NSW, Australia). Coverslips were sealed with nail polish. For controls, primary antibodies were deleted, and no signal was detected.

For immunolabelling experiments involving microfilaments, several further steps were required. First, root tips were pre-treated for 10 min with PME (in which Triton X-100 was not included) containing 400 µM maleimidobenzoyl N-hydroxysuccinimide ester (MBS; Pierce, Rockford, IL, USA), a mild protein cross-linker that helps stabilise microfilaments. Second, the fixative was modified by the inclusion of both 400 µM MBS and 1.0% glutaraldehyde. And third, aldehyde-induced autofluorescence was minimised by treating slides with 1 mg ml<sup>-1</sup> sodium borohydride in PBS, following the initial PBS rehydration step, followed by PBS washes (3×5 min). While these modifications affected neither peroxisome nor microtubule labelling, they induced significant amounts of autofluorescence even after sodium borohydride treatment and were only used when observations of microfilaments were required.

Immunolabelling of tobacco BY-2 cells, leek epidermal cells and *Arabidopsis* whole roots followed standard protocols (Collings et al. 1998, 2002).

#### Transient expression of peroxisomal GFP in leek epidermal cells

Mature leek plants were trimmed of green leaves, leaving only the lower 5 cm of the leaves and the roots, and then split in half with a razor blade. The youngest, central leaves were removed from the base to expose the inner epidermis of the last leaf in which the ligule remained present. The leek was then transformed with a particle bombardment system (model PHS-1000, 1,100-psi rupture discs; Bio-Rad). Plasmid DNA (0.2–0.5 µg) encoding GFP fused to the carboxy-terminal tripeptide -SKL, the prototypic PTS1, was prepared and coated onto gold particles (1.0 µm diameter; Bio-Rad, Regents Park, NSW, Australia) as described previously (Collings et al. 2002). Halved leek plants were then stood in water to recover and express peroxisomal-targeted GFP for 42–66 h, before being observed by confocal microscopy. During this time, the inner leek leaves elongated by several centimetres.

#### Confocal microscopy

Immunolabelled root cells were imaged on a confocal microscope (SP2 system; Leica, Wetzlar, Germany) using either a combination of confocal and two-photon microscopy (SU; Sydney University) or confocal microscopy with a UV laser (ANU; Australian National University). Using either 40× or 100× NA 1.4 oil immersion lenses, stacks of optical sections were collected with 0.5-µm steps, with the multiple wavelengths recorded for each plane using an average of four to six passes. Because of bleed-through problems, DAPI fluorescence was collected sequentially from the other fluorophores. DAPI-labelled DNA was imaged (SU) in two-photon mode using 800-nm excitation

from a Mira tuneable, pulsed titanium sapphire laser (Coherent, Santa Clara, CA, USA). Fluorescence was collected through an NA 1.4 oil immersion condenser by a transmitted light detector from 400 to 560 nm. Alternatively (ANU), DAPI-labelled DNA was imaged by excitation with a UV laser (model Enterprise II 651; Coherent) at 361 nm, with fluorescence collected confocally with emission windows set from 400 to 480 nm. Fluorescence was then collected concurrently using conventional confocal microscopy. Following excitation with 488-nm argon, and 543- and 633-nm helium/neon lasers, fluorescence was collected using windows generally set to 500–530 nm for FITC and Alexa 488, 560–620 nm for Cy-3 and Alexa 546, and above 645 nm for Cy-5. Bleed-through of the FITC and Alexa 488 signals into red emission wavelengths was minimised by running the 488-nm laser at reduced power, while running the 543- and 633-nm lasers at full power.

GFP expression in whole mounted leek leaves was imaged using a 20× NA 0.7 water-immersion lens, with excitation at 488 nm and fluorescence collected from 500 to 550 nm. Transmitted light images were collected concurrently.

All images were processed with Adobe Photoshop version 5.0 (Adobe, San Jose, CA, USA).

#### Electron microscopy

The tips from onion roots were excised on a drop of 6% glutaraldehyde in 50 mM Pipes buffer (pH 7.2) on dental wax, and transferred to a larger volume of the same fixative in 20-ml scintillation vials (2 h). After two 15-min 100 mM cacodylate washes, the root tips were fixed in 2% osmium tetroxide in 100 mM cacodylate buffer (2 h), rinsed briefly in water and stained en bloc with 2% uranyl acetate overnight at 4 °C. After several water rinses at room temperature, the samples were dehydrated in an acetone series, transferred to propylene oxide, and embedded in a 1:1 mixture of Spurr's and epon resin. When a 75% resin solution was reached, the final 25% of propylene oxide was allowed to evaporate from the resin mix by affixing pieces of aluminium foil to the top of the scintillation vial with pin holes in the top. This allowed a very gradual increase in the percentage of plastic and occurred over 18–24 h. Fresh resin was added to the samples, the vial caps returned, and the specimens were shaken on a rocking platform for 24 h. The root tips were then flat embedded in BEEM embedding moulds and the resin polymerised at 68 °C in a vacuum oven. The specimens were cut from the embedding moulds with a jeweller's saw and oriented on acrylic rods so that sections would be made in the long axis of the root. Initially, sections were cut at 0.35 µm with a Delaware Histoknife and stained with 1% toluidine blue in 1% sodium borate to determine the presence of cells in telophase. When cells in telophase were detected, the block face was sectioned with a Reichert Ultracut ultramicrotome to give sections of approximately 100 nm thickness. The sections were mounted on 300-mesh copper grids and post-stained with 2% uranyl acetate (5 min) and Reynold's lead citrate for 7 min. Sections were observed with a Zeiss EM 10 CR electron microscope at 60 kV.

## Results

### Immunofluorescent localisation of peroxisomes to the cell plate

In Fig. 1, false-colour images show the localisation of peroxisomes in median confocal sections through interphase and dividing cells isolated from the primary meristem of onion roots. Peroxisomes were visualised with polyclonal anti-catalase (green), microtubules with monoclonal anti-tubulin (red) and DNA with DAPI-labelling (blue). During interphase, peroxisomes

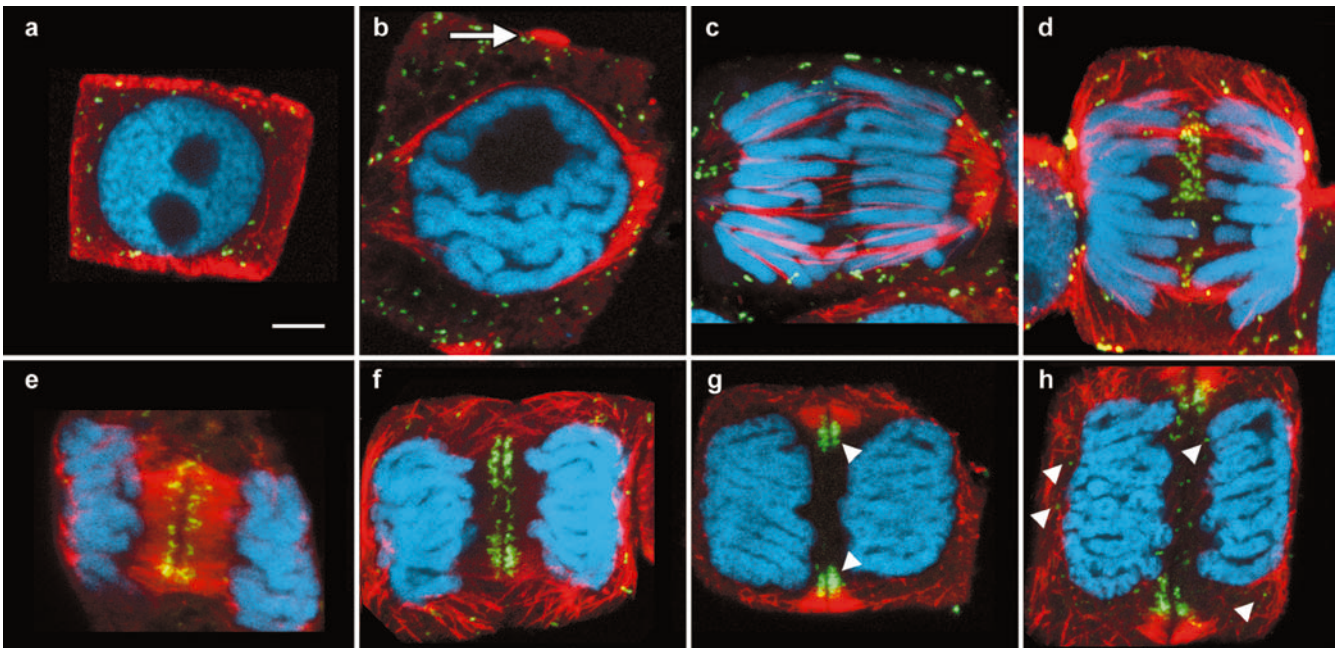


**Fig. 1a–h** Peroxisomes localise to the inner edge of the expanding microtubule phragmoplast. Isolated onion (*Allium cepa*) root meristem cells demonstrate changes in microtubules and peroxisome localisation through the division cycle. These false-colour images, which show microtubules (red), DAPI-labelled DNA (blue) and peroxisomes (green; areas of peroxisome co-localisation with microtubules appear yellow) are confocal median sections through the centre of the cell, with each image being a maximum projection of four sequential optical sections collected at 0.5- $\mu$ m intervals. Microtubules occurred in their normal configurations through the cell cycle. **a** Interphase; peroxisomes are random through the cytoplasm and transverse microtubules are restricted to the cell cortex. **b** Prophase; while peroxisomes remain random, cortical microtubules have depolymerised and formed into the preprophase band (arrow) and the beginnings of the mitotic spindle. The nuclear envelope has not yet broken down. **c** Early anaphase; soon after chromosome separation, peroxisomes remain randomly distributed and are excluded from the spindle. **d** Late anaphase; peroxisomes gather at the division plane forming a continuous band. The spindle is still present and the phragmoplast has not yet developed. **e–h** Early to late telophase; in early telophase, the microtubules of the phragmoplast form a complete disc, with peroxisomes present in two zones immediately on either side of where the microtubule arrays intersect (**e**). In mid-telophase, the microtubule phragmoplast has begun to expand outwards towards the parent cell wall, but the peroxisomes are still present in two complete, disc-like zones inside the microtubule ring (**f**). **g** By late telophase, peroxisomes are present in a ring at the inner edge of the phragmoplast, inside the microtubules ring (arrowheads). **h** From late telophase to early  $G_1$  phase, the microtubules begin repolymerising, and peroxisomes have begun to move away from the division site (arrowheads). Bar in **a** = 5  $\mu$ m for all images

distribute randomly throughout the cytoplasm while microtubules are confined to the cell cortex (Fig. 1a). During division, peroxisomes remain randomly spaced from prophase (Fig. 1b) until early anaphase, although they are excluded from the mitotic spindle (Fig. 1c). However, late in anaphase, but prior to the appearance of phragmoplast microtubules, peroxisomes aggregate into a single band at the midpoint of the spindle (Fig. 1d). By the onset of telophase, almost all

peroxisomes within the cell occur at the centre of the phragmoplast. The single band of peroxisomes, found in late anaphase, splits into two parallel bands found on either side of the developing cell plate (Fig. 1e). As telophase progresses, microtubules in the phragmoplast progress from a disc-like configuration into a ring, through a combination of outward expansion and microtubule depolymerisation at the centre of the phragmoplast. Initially, the outward expansion of the two peroxisomal bands is delayed so that the ring of microtubules surrounds the two parallel layers of peroxisomes adjacent to the developing cell plate (Fig. 1f). Eventually, as the cell plate expands out towards the parent cell wall, peroxisomes also redistribute outwards forming two concentric peroxisomal rings that occur immediately inside the expanding microtubule phragmoplast on either side of the cell plate (Fig. 1g). As telophase ends and  $G_1$  phase begins, phragmoplast microtubules begin to depolymerise and the interphase array redevelops. At this stage, the strict localisation of peroxisomes, evident throughout telophase, begins to break down with peroxisomes moving away into the cytoplasm (Fig. 1h; arrowheads).

Because of the differences between microtubule and peroxisome localisations during the cell cycle, we also investigated the relative localisation of actin microfilaments with respect to peroxisomes and microtubules. Although triple-labelling experiments were attempted, technical problems prevented concurrent labelling of peroxisomes along with both microtubules and microfilaments. Therefore, the images in Fig. 2 show microfilaments co-localised with either peroxisomes (Fig. 2a–f) or microtubules (Fig. 2g–l) for the three specific stages of division important for peroxisome aggregation, late anaphase, early telophase and late telophase. Interphase cells, and the early stages of mitosis are not shown,

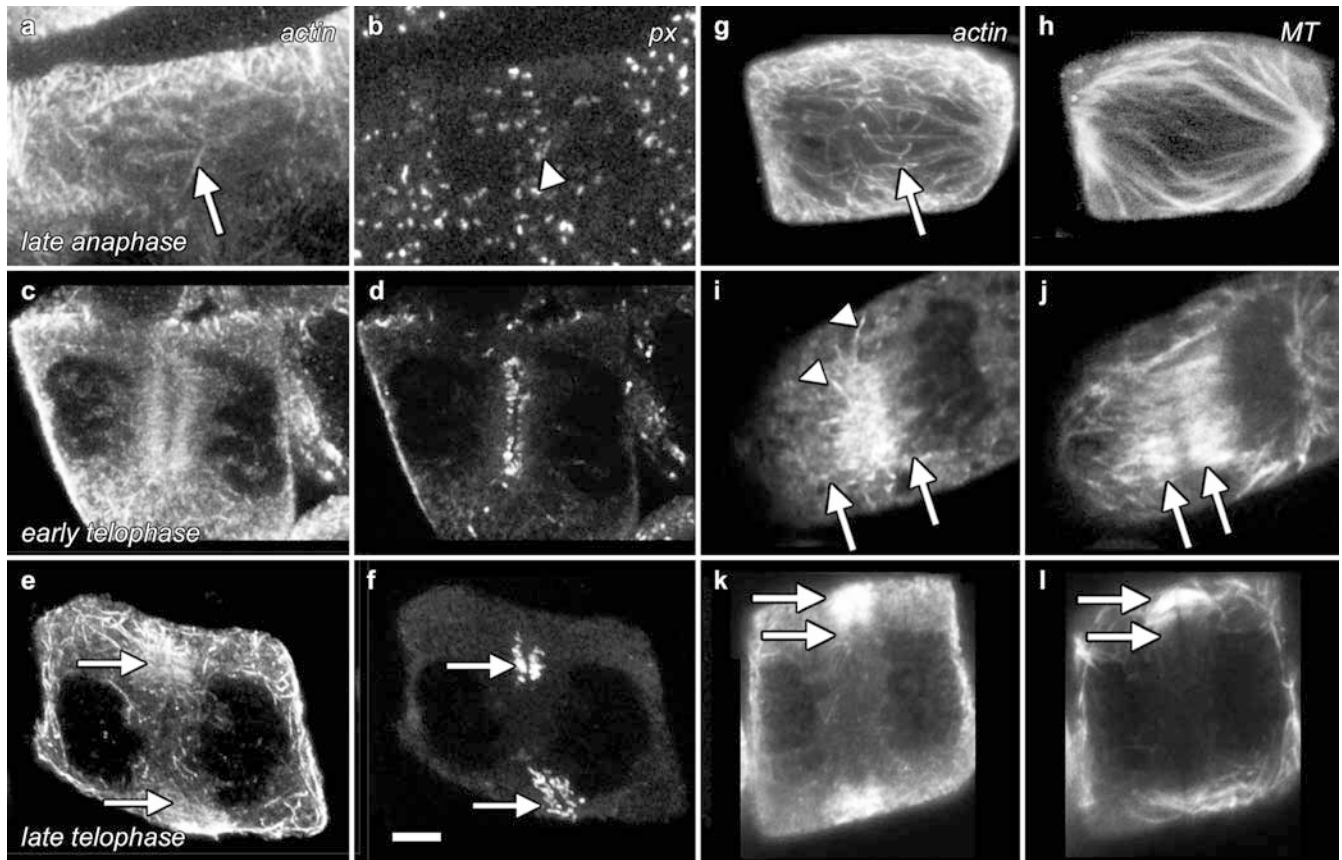


**Fig. 2a–l** Comparative localisations of the microfilament cytoskeleton with peroxisomes and microtubules during cell division of onion root meristem cells. All images are shown in pairs, with microfilaments (*actin*) either double-labelled with peroxisomes (*px*) or microtubules (*MT*). Images are median sections through the centre of the cells, are projections of four confocal optical sections taken at 0.5- $\mu\text{m}$  intervals, and are presented at three stages of the cell cycle; late anaphase (**a, b, g, h**), early telophase (**c, d, i, j**) and late telophase (**e, f, k, l**). **a, g** An extensive microfilament cytoskeleton remains in the cortex of the cell through cell division, and although microfilaments are excluded from the mitotic spindle, during late anaphase microfilaments develop at the centre of the spindle between the departing chromosomes (*arrows*). In the cortex, there is no evidence for a zone of actin depletion that marks the future plane of cell division. **c, i** During early telophase, two parallel discs of phragmoplast microfilaments occur. Microfilaments connect outward from the phragmoplast towards the plasma membrane (**i**; *arrowheads*). **e, k** By late telophase, the microfilament phragmoplast is toroidal, appearing as bands on either side of a median-sectioned cell. **a, b** Late anaphase; a band of peroxisomes (**b**, *arrowhead*) begins to occupy the space between the separating chromosomes around the same time as microfilaments (**a**, *arrow*). **c, d** Early telophase; phragmoplast microfilaments co-localise with two parallel bands of peroxisomes. **e, f** Late telophase; peroxisomes occur in a ring which coincides with the inner edge of the microfilament phragmoplast (compare identically placed *arrows*). **g, h** Late anaphase; while microtubules are restricted to the mitotic spindle, microfilaments occur in the central regions of the spindle (*arrow*). **i, j** Early telophase; the microfilament bundles in the phragmoplast are consistently shorter than the phragmoplast microtubules. *Arrows* in the microfilament image (**i**) show the width of the microtubule phragmoplast, and vice versa in **j**. **k, l** Late telophase; in the laterally expanded phragmoplast, where microtubules and microfilaments have depolymerised in the centre, microfilaments remain shorter than the microtubules, and extend further inwards towards the cell plate than do the microtubules (compare identically placed *arrows*). Bar in **f** = 5  $\mu\text{m}$  for all images

although in such cells, peroxisomes distribute randomly through the cytoplasm and show some co-alignment with the extensive microfilament arrays (data not shown). Similarly, a comparison of microfilament and microtubule patterns during interphase showed that interphase cells contained randomly distributed microfilaments throughout the cytoplasm, but that transverse cortical microtubules and microfilaments occur adjacent to the plasma membrane (data not shown; see McCurdy et al. 1991; Liu and Palevitz 1992).

For these three important stages of peroxisome localisation, we first discuss the organisation of actin microfilaments. In late anaphase, microfilaments begin to invade the cell division plane between the separating chromosomes, even as they remain excluded from the space around the chromosomes themselves. Typically, these microfilaments are randomly distributed, with a bias towards being transverse. (Fig. 2a, g; *arrows*). By early telophase, an extensive microfilament phragmoplast develops, which appears as two discs of microfilaments separated by a dark band where the cell plate forms (Fig. 2c, i). This band, although present, is less prominent in Fig. 2i than Fig. 2c. Microfilaments also often bridge laterally from the phragmoplast towards the plasma membrane (Fig. 2i; *arrowheads*). But by late in cytokinesis, the microfilament phragmoplast has expanded towards the edge of the cell and now forms a ring, which in optical sections appears as a pair of bands at the edge of the cell (Fig. 2e, k).

Peroxisomes show similar a distribution to microfilaments. In late anaphase, peroxisomes begin to invade the cell division plane at around the same time that actin microfilaments (Fig. 2b; arrowhead). Similarly, in early telophase, the two parallel discs of peroxisomes on either side of the cell plate match the localisation of actin (Fig. 2d). And in late telophase, peroxisomes also colocalise with microfilaments at the inner edge of the phragmoplast (Fig. 2e, f; arrows), which is different from the separation found between peroxisomes and microtubules (for example, Fig. 1f–h).

In contrast, differences occur between microtubule and microfilament organisation during the formation and lateral expansion of the phragmoplast (Fig. 2i–l). During early telophase, when the phragmoplast microtubules form a disc, the microtubules are longer than the microfilaments of the phragmoplast (Fig. 2i, j; compare arrows). During the later stages of cytokinesis, when the microtubule phragmoplast forms an annulus, microfilaments are also organised in a subtle but significantly different way, for when the phragmoplast is viewed in cross-section, microfilaments extend further into the cell (Fig. 2k, l; compare arrows).

#### Electron microscopy shows aggregated peroxisomes during cytokinesis

Electron micrographs show that interphase cells of onion roots generally contain randomly distributed peroxisomes that are typical of the unspecialised peroxisomes present in other non-photosynthetic tissues not involved in oil storage (Huang et al. 1983). One exception to this random distribution occurs in the presence of lipid bodies. Lipid bodies are present in many cells, most notably those towards the apex of the root which are developmentally less mature, and often occur in close association with unspecialised peroxisomes in a similar way to the glyoxysome-type peroxisomes found in oil seeds (data not shown).

In contrast to the generally random distribution of peroxisomes in interphase cells, our electron-microscope observations of several hundred telophase cells show that in every case, peroxisomes aggregated adjacent to the cell plate (Fig. 3). This confirms our observations by immunofluorescence. In median sections (100 nm) of both early (Fig. 3a, b) and late telophase (Fig. 3c, d) cells, numerous peroxisomes occur on either side of the nascent cell plate. In the early stages of division, where the cell plate has yet to condense, microtubules and peroxisomes are interspersed (Fig. 3a, b). However, by late telophase, most peroxisomes (Fig. 3c; arrowheads) localise to just the inside of the site of vesicle fusion, where the cell plate is probably quite fluid (Fig. 3c; arrows). The central areas of the cell plate, which have likely undergone stiffening, have no adjacent peroxisomes (Fig. 3c; cp). Unfortunately, as yet neither chemical fixation protocols nor freeze-substitution methods have given reliable preservation of actin microfilaments in onion root cells.

Aggregated peroxisomes range in size from 0.3 to 0.5  $\mu\text{m}$  in length, and vary from being globular to tear-drop- and dumb-bell-shaped. Often the ends of the peroxisomes associate with smooth ER, but no inclusions are visible inside them. However, horseshoe-shaped peroxisomes also occur that contain a central cavity (Fig. 3a, d; asterisks), which is often, but not always, filled with a vesicle (Fig. 3e, f). These vesicles are somewhat larger than the secretory vesicles generally involved in cell plate formation, and their membrane is often closely appressed to the peroxisomal membrane forming a double membrane (Fig. 3e, f; arrow). Further structures are sometimes seen within the vesicles (Fig. 3e; arrowhead).

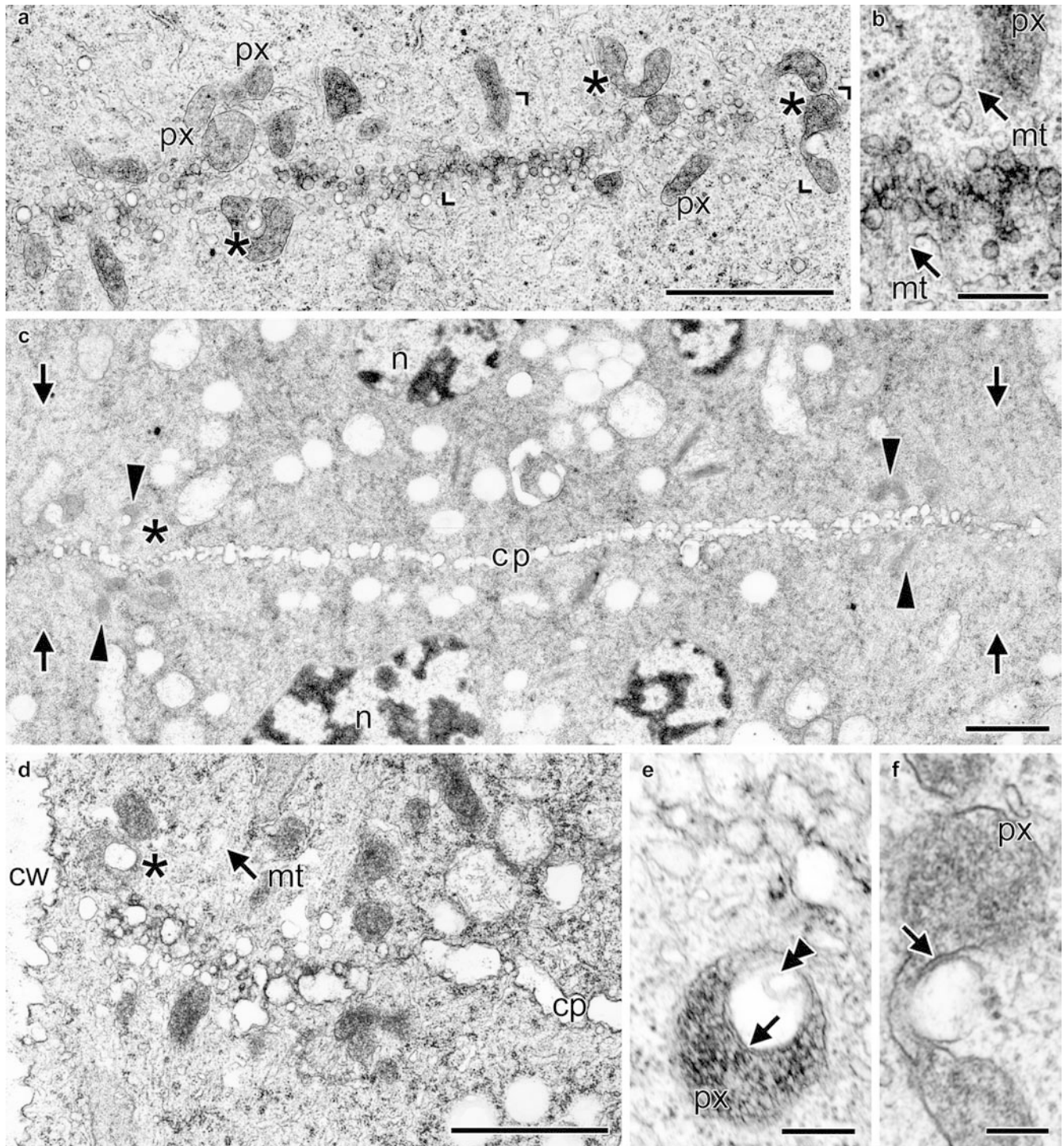
#### Inhibitor studies demonstrate that peroxisomal aggregation depends on microfilaments and myosin

Agents that block the interaction of microfilaments and myosin prevent the aggregation of peroxisomes (Fig. 4). Treatment of root apices with cytochalasin D (5  $\mu\text{M}$ ) for 3 h disrupts the microfilament cytoskeleton (Fig. 4b) but not microtubules (Fig. 4a). Cytochalasin also dramatically alters peroxisomal distribution, so that peroxisomes remain random at the time of cytokinesis (Fig. 4c) even though microtubules still form the phragmoplast (Fig. 4d). The actin monomer-sequestering drug latrunculin B (2  $\mu\text{M}$ , 3 h) also disrupts microfilaments (data not shown) and causes randomisation of peroxisomes during cytokinesis (Fig. 4e, f). Similarly, the putative myosin inhibitor 2,3-butanedione monoxime (BDM; 30 mM, 3 h), an agent that reduces or inhibits peroxisome movement in interphase *Arabidopsis* cells (Jedd and Chua 2002; Mathur et al. 2002), randomises peroxisomes during telophase (Fig. 4g, h), although it disrupts neither microfilaments nor microtubules (data not shown). These three inhibitors have variable effects, with some dividing cells showing incomplete randomisation of peroxisomes, and partial aggregation at the cell plate. However, control treatments in which roots are immersed in water for 3 h, always show aggregated peroxisomes (Fig. 4i, j).

As further controls for these microfilament- and myosin-disrupting agents, two additional drugs that inhibit cell plate growth and expansion were tested. Dichlobenil (dichlorobenzonitrile) is a herbicide that inhibits cellulose synthesis and blocks cell plate formation in onion roots (Vaughn et al. 1996) while caffeine blocks vesicle fusion within the phragmoplast, preventing cell plate formation and expansion (Valster and Hepler 1997). At concentrations that inhibit cell plate formation, neither dichlobenil (10 mM) nor caffeine (5 mM) modifies aggregation of peroxisomes adjacent to the microtubule phragmoplast (data not shown).

#### Immunolocalisation of peroxisomes during cytokinesis in other tissues and plants

We have observed aggregation of peroxisomes adjacent to the cell plate in the roots of several monocot species,



including leek and *Crinum* (data not shown). Aggregation also occurs in the large epidermal cells of immature leek leaves, although unlike the smaller root cells, aggregation is often incomplete with some peroxisomes remaining in the cytoplasm away from the cell plate (Fig. 5a, b). However, in *Arabidopsis* roots grown on agar plates containing Hoagland's media, peroxisomes remain randomly distributed through the cytoplasm (Fig. 5c, d), as they did in *Arabidopsis* and *Brassica* roots germinated on paper moistened with

distilled water (data not shown). Our immunofluorescence results with *Arabidopsis* roots are consistent with published reports of peroxisomal distributions in living *Arabidopsis* roots where aggregations of peroxisome adjacent to the cell plate have not been described (Cutler et al. 2000; Jedd and Chua 2002; Mano et al. 2002; Mathur et al. 2002). In tobacco BY-2 cells, many peroxisomes associate with the outer edge of the microtubule phragmoplast (Fig. 5e, f). Electron micrographs of dividing BY-2 cells show similar



**Fig. 3a–f** Electron micrographs confirm that peroxisomes associate with the developing cell plate in onion root meristem cells. **a** A section through a developing cell plate in early telophase showing vesicles fusing into an incomplete wall. Numerous (at least 13) peroxisomes (*px*) stain more heavily than other organelles, and are interspersed among the microtubules on either side of the developing plate. **b** Enlargement of the cell plate region boxed in **a**, with microtubules clearly visible (*mt* and *arrow*) adjacent to a peroxisome. **c** A late telophase cell, at approximately the same stage as Fig. 1g. Peroxisomes aggregate in two regions (*arrowheads*) towards the outer edge of the expanding cell plate (*cp*), but immediately inside the sites of vesicle fusion. These regions, marked with *arrows* exclude most large organelles, including peroxisomes, but contain phragmoplast microtubules (not visible at low magnification). Chromatin within the nuclei (*n*) has begun to recondense. **d** A higher magnification image showing a late-stage phragmoplast as it nears the parent cell wall (*cw*). Peroxisomes occur to the inside of the band of phragmoplast microtubules (*mt* and *arrow*), consistent with immunofluorescence images. **e** Many peroxisomes aggregated at the cell plate are horseshoe-shaped and often show association with large vesicles (*asterisks* in **a** and **d**). This example shows a vesicle containing a peculiar, membrane-bound tail (*double arrowhead*). **f** Enlargement of the peroxisome-vesicle association boxed in **a**, with appression of the vesicle membrane to the peroxisome membrane clearly visible (*arrow*). Bars = 1  $\mu\text{m}$  (**a**, **c**, **d**), 0.2  $\mu\text{m}$  (**b**, **e**), 0.1  $\mu\text{m}$  (**f**)

localisations and examples of peroxisomes associated with vesicles (data not shown).

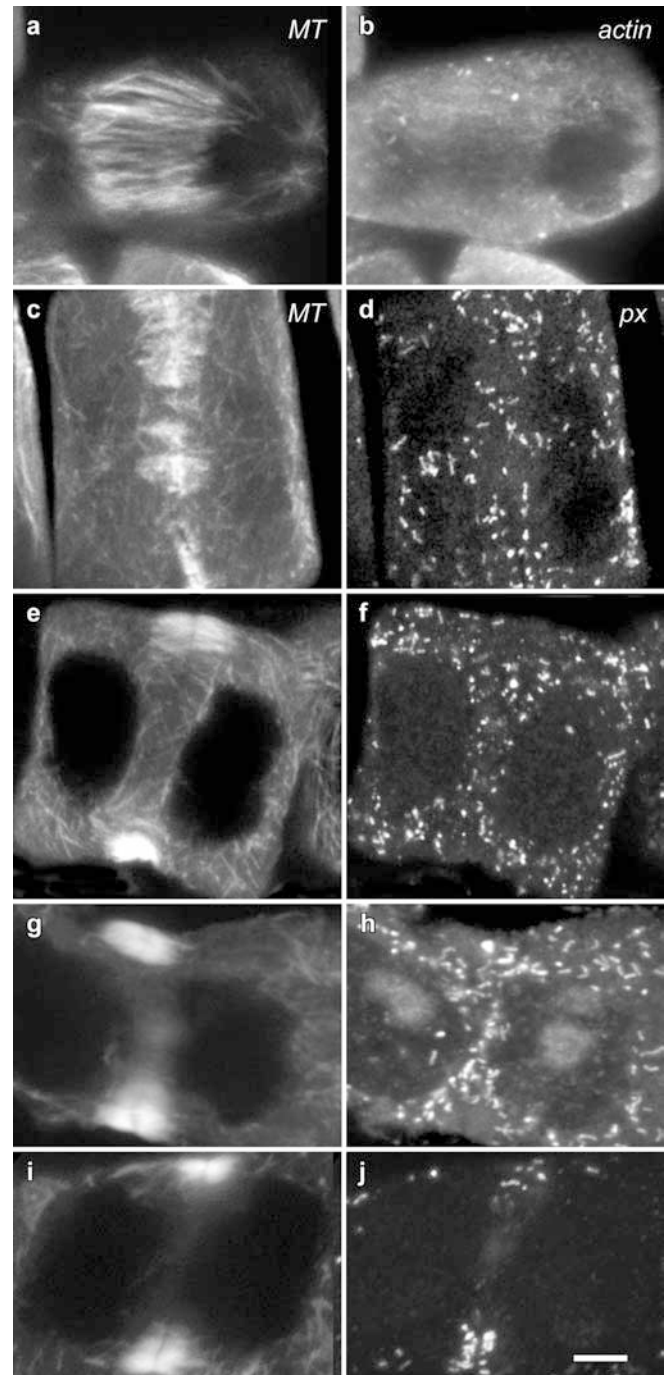
#### Targeted-GFP confirms peroxisomal aggregation during cytokinesis in leek epidermal cells

Immunofluorescence experiments (see Fig. 5a, b) showed that cell divisions occur towards the base of immature leek leaves. Therefore, we modified our particle-bombardment methods, previously used to express peroxisomal-targeted GFP in the non-dividing epidermal cells of mature leek leaves (Collings et al. 2002), to transform cells in the immature leaves found towards the centre of halved leek plants. Wherever aggregates of peroxisomes occur in immature leaves, concurrent bright-field images show dividing cells (Fig. 6), whereas interphase cells always show randomly distributed peroxisomes (data not shown; see Collings et al. 2002).



**Fig. 4a–h** Aggregation of peroxisomes in onion root meristem cells does not occur when microfilaments are disrupted or myosin is inhibited. **a**, **b** Microfilaments (*actin*) and microtubules (*MT*) were double-labelled in onion roots that were treated for 3 h with cytochalasin D (5  $\mu\text{M}$ ). This treatment almost completely eliminated polymerised actin microfilaments, leaving only short stubs in the cytoplasm (**b**) while the microtubules in an early phragmoplast remain unaffected (**a**). **c–j** Microtubules (*MT*) and peroxisomes (*px*) were double-labelled. **c**, **d** Cytochalasin D (5  $\mu\text{M}$ , 3 h) blocks peroxisome aggregation leaving peroxisomes randomly distributed, but does not overly affect the formation of the microtubule phragmoplast. **e**, **f** Latrunculin B (2  $\mu\text{M}$ , 3 h), which disrupts microfilaments in a similar way to cytochalasin, randomises peroxisomes in a similar way to cytochalasin. **g**, **h** The putative myosin inhibitor 2,3-butanedione 2-monoxime (BDM, 30 mM, 3 h) randomises peroxisomes. **i**, **j** Control treatments, in which onion root tips were immersed in water for 3 h show normal aggregation of peroxisomes. All images are median sections that are maximum projections of four individual optical sections taken at 0.5- $\mu\text{m}$  intervals. Bar in **j** = 5  $\mu\text{m}$  for all images

In epidermal cells during late telophase, peroxisome aggregates (Fig. 6a–f) appear similar to those seen in the same cells with immunofluorescence (Fig. 5a, b). Most peroxisomes formed into two parallel bands that ringed the outer edge of the dividing cells, although as seen with immunofluorescence, aggregation is not always complete. Peroxisomes within the aggregates were generally stationary, whereas those in other parts of the cytoplasm remained highly dynamic (data not shown). Aggregates of peroxisomes are unstable, with the banding pattern breaking down in under 20 min (Fig. 6g–l), although there was no indication from concurrent bright-field



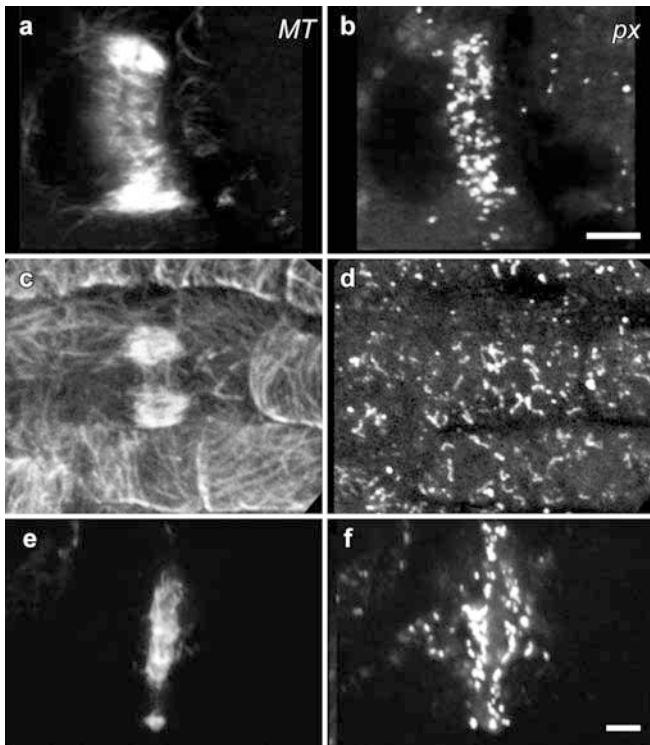


**Fig. 5a–f** Aggregation of peroxisomes occurs in leek (*Allium porrum*) epidermal and tobacco (*Nicotiana tabacum*) BY-2 cells, but not in *Arabidopsis thaliana*. Microtubules (MT) and peroxisomes (px) were double-labelled and are shown in paired, median sections that are maximum projections of four individual optical sections taken at 0.5- $\mu$ m intervals. Images show leek epidermal cells (a, b), epidermal cells viewed in whole-mounted *Arabidopsis* roots (c, d) and tobacco BY-2 cells (e, f). a, b Aggregated peroxisomes during division in leek epidermal cells, demonstrating that the process of aggregation is not limited to cell divisions within the root. c, d *Arabidopsis* root epidermal cells show random peroxisomes during all stages of the cell cycle, including cytokinesis. e, f Tobacco BY-2 cells show some aggregation of peroxisomes during cell division, but in this case, the peroxisomes are found at the outer edge of the microtubule phragmoplast. Bar in b = 5  $\mu$ m for a–d; bar in f = 5  $\mu$ m for e and f

images that cytokinesis had been completed. Therefore, we do not yet know whether the rapid loss of aggregation indicates the end of cytokinesis, or whether it occurs as a result of the laser light irradiation.

## Discussion

The dramatic alignment of peroxisomes associated with the cell plate and phragmoplast of dividing onion root cells has not previously been described in higher plants using fluorescence microscopy. The recent studies with GFP targeted to peroxisomes (Cutler et al. 2000; Jedd and Chua 2002; Mano et al. 2002; Mathur et al. 2002) did not discuss cell division, and were conducted in *Arabidopsis* roots, a tissue where peroxisomes do not aggregate. All previous descriptions of peroxisomes aligning during cell division have been with electron microscopy, and moreover, such observations have been

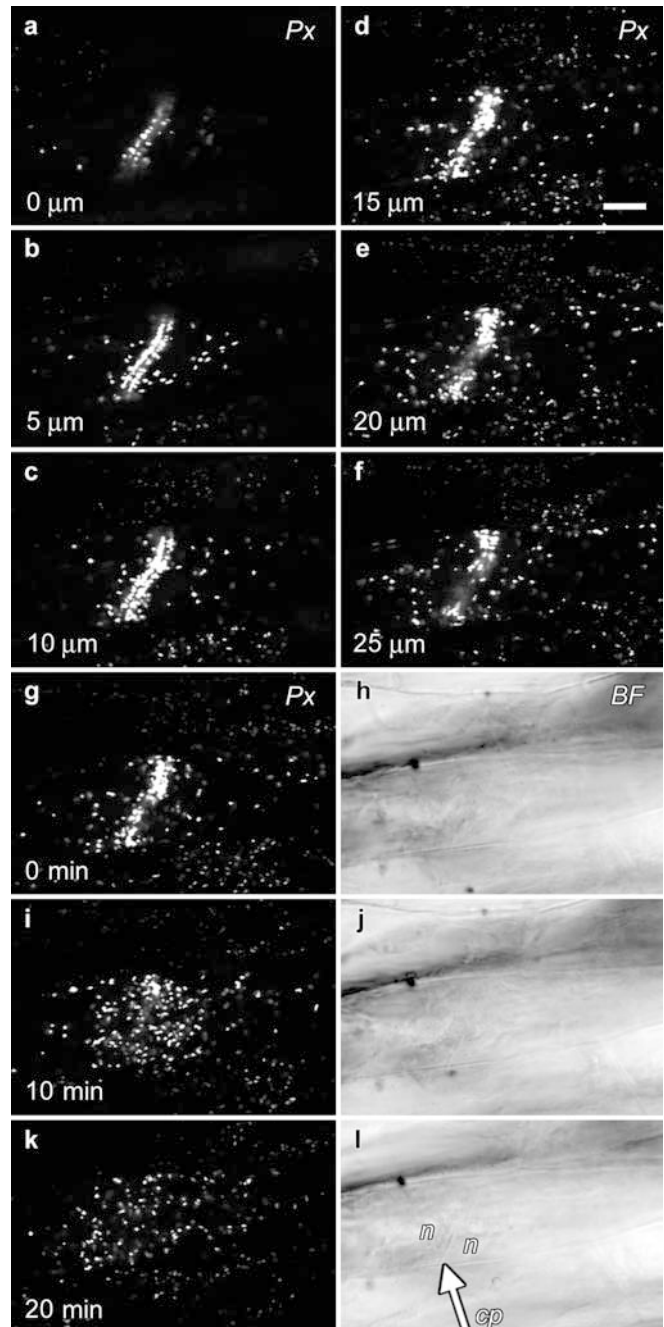


**Fig. 6a–l** Aggregation of peroxisomes in living leek epidermal cells, as visualised with a GFP fusion protein. Immature leek epidermal leaves were transformed by particle bombardment with a construct that expressed peroxisomal-targeted GFP. After incubation of the stem bases for 42–66 h, high levels of GFP were observed by confocal microscopy in many peroxisomes (Px). In some cases, these were aggregated, and concurrent bright-field images (BF) showed these to be dividing cells. a–f Optical sections at 5- $\mu$ m intervals (depths indicated at lower left of images) through an epidermal cell in late telophase showing peroxisomes aggregated into two distinct bands. g–l A time-course of peroxisome movement in the same cell, beginning at 0 min with an image taken from the optical series (17.5  $\mu$ m), and with subsequent images at 10 and 20 min. Outlines of the cell plate (cp) and daughter nuclei (n) are visible in the concurrent bright-field images, although as these bright-field images were made in whole-mount specimens, it was more difficult to visualise the cell plate formations. Bar in d = 10  $\mu$ m for all images

scarce. The novel organelles that were observed near the developing cell plate of dividing onion root cells (Porter and Machado 1960), prior to the first description of peroxisomes in plants, were subsequently confirmed to be peroxisomes (Hanzely and Vigil 1975), while electron micrographs of guard mother cell divisions in onion cotyledons appear to show peroxisomes aggregated near the cell plate (Palevitz and Hepler 1974).

Peroxisomes also align at the site of cell division in numerous lower plants. In such cells, both plastid division and the division of a single peroxisome associated with the plastid are synchronised with cell division (Brown and Lemmon 1990) by aligning the plastid and peroxisome at the plane of cell division. For example, the single elongated peroxisome of the alga *Klebsormidium* lies between the nucleus and the chloroplast, and during cytokinesis the cleavage furrow forces the peroxisome into the gap formed in the dividing plastid, causing the peroxisome itself to divide (Pickett-Heaps 1972). Peroxisomal division is also linked to plastid division during cytokinesis of the hornworts *Phaeoceros* and *Notothylas* (Brown and Lemmon 1985) and in developing meiospores of the moss *Funaria* (Busby and Gunning 1988), while in the red alga *Cyanidioschyzon* the single peroxisome associates and divides with both the plastid and mitochondrion (Miyagishima et al. 2001). These divisions are fundamentally different from the alignment of peroxisomes in onion, for they involve the alignment, division and partitioning of single peroxisomes at the cell division plane. Onion cells may contain several hundred peroxisomes, and do not have this restriction.

#### Peroxisome aggregation depends on microfilaments and myosin

During mitosis and cytokinesis, peroxisome distribution is microfilament- and myosin-dependent. Not only do peroxisomes always co-localise with microfilaments (and not microtubules) when they aggregate during cytokinesis, but two drugs that disrupt microfilament organisation (cytochalasin and latrunculin) also prevent peroxisome aggregation. The putative myosin antagonist, BDM, which inhibits myosin-dependent cytoplasmic streaming and peroxisome movement in interphase plant cells (Jedd and Chua 2002; Mathur et al. 2002) and disrupts microfilament-dependent cell plate expansion (Molchan et al. 2002), also prevents aggregation even though the efficacy of BDM as a specific myosin antagonist has been questioned (Ostap 2002).

These data are also consistent with the rapid streaming of peroxisomes in interphase cells (up to  $6 \mu\text{m s}^{-1}$ ) which is reversibly inhibited by microfilament-destabilising drugs (Collings et al. 2002; Jedd and Chua 2002; Mano et al. 2002; Mathur et al. 2002). Peroxisome velocities are consistent with plant myosins characterised in vitro (Yamamoto et al. 1999), and with examples of plant-myosin-controlled organelle transport such as the

ER and Golgi apparatus (Boevink et al. 1998). Myosin has also been immunolocalised adjacent to the phragmoplast in dividing onion root cells (Parke et al. 1986). It would seem highly probable, therefore, that peroxisomes translocate along the microfilament bundles using myosin motors.

#### Peroxisomes through the cell cycle in onion root cells

Our idea for how peroxisomes localise to the cell plate in onion cells is based on our observations and numerous studies on onion root tips (McCurdy et al. 1991; Liu and Palevitz 1992; Giménez-Abián et al. 1998). This model need not, however, hold true for other systems in which plant division is often studied, as the assumption that all plant cell divisions are identical is not valid, as shown by the variations found in cytokinesis in endosperm and gametophytic cells (Otegui and Staehelin 2000), and by the differences we see between peroxisome distribution in onion and *Arabidopsis*.

We propose that late in anaphase, but before the phragmoplast develops, microfilament bundles form at the spindle's equator. Peroxisomes translocate along these bundles, but some localised signal inactivates their movement when they reach the future location of the cell plate, resulting in aggregation of the peroxisomes into a single band. The nature of this signal is uncertain. In interphase cells, however, GFP targeted to peroxisomes shows that individual peroxisomes alternate between rapid streaming and being stationary, presumably because either the myosin motor is turned off or the peroxisome has detached from the microfilament cytoskeleton (Collings et al. 2002; Jedd and Chua 2002; Mano et al. 2002; Mathur et al. 2002). Our preliminary observations of cytokinetic cells with GFP targeted to peroxisomes also suggest this, with peroxisomes adjacent to the phragmoplast being comparatively stationary, and peroxisomes elsewhere within the cell being more dynamic.

During telophase, the phragmoplast comprises parallel microtubules and microfilaments, with the plus- or barbed-ends of actin microfilaments towards the centre (Kakimoto and Shibaoka 1988), although for unknown reasons microfilaments do not extend as far from the equatorial plane as the microtubules do (Kakimoto and Shibaoka 1988; Liu and Palevitz 1992; Zhang et al. 1993; this study). The dense network of phragmoplast microtubules excludes most organelles, but not peroxisomes, most likely because the peroxisomes were already in this location with the microtubules polymerised between them, and because of continued peroxisome interactions with microfilaments. Furthermore, the distribution of peroxisomes into two parallel layers on either side of the exclusion zone is consistent with myosin motors trafficking peroxisomes to the plus-ends of the microfilament bundles. As the phragmoplast matures, both microtubules and microfilaments polymerise at its outer edge but, initially, only microtubules depolymerise at the centre so that the annulus

of the microtubules overlies and surrounds a microfilament disc. This observation on fixed material is consistent with microinjection-based observations in *Tradescantia* stamen hairs (Zhang et al. 1993), and with observations of fixed *Arabidopsis* roots (data not shown). Peroxisomes remain associated with the actin microfilament cytoskeleton but unlike the young phragmoplast where peroxisomes were interdispersed amongst the microtubules, peroxisomes are excluded from the newly polymerised parts of the phragmoplast because there is no pre-existing aggregation of peroxisomes. However, as the phragmoplast matures further, microfilaments also depolymerise at its centre (this study; Liu and Palevitz 1992), and peroxisomes redistribute outwards to form a ring. Importantly, the microfilament annulus is broader than that of the microtubules, which allows for the peroxisomes to colocalise with microfilaments on the inner edge of the microfilament phragmoplast where there are no microtubules.

#### The function(s) of peroxisomes during cytokinesis

Peroxisome aggregation does more than simply ensure peroxisomes partition correctly into the daughter cells during division. In animal cells, organelles not required for division, including mitochondria, the Golgi apparatus and peroxisomes, distribute and partition into daughter cells randomly (Warren and Wickner 1996). Similarly, organelles not required for plant cell cytokinesis, such as mitochondria, also distribute randomly during division (Nebenführ et al. 2000). However, organelles required by plants for cell plate formation, such as ER and the Golgi apparatus accumulate in the plane of cell division, although this accumulation is only partial with both ER and the Golgi remaining at other sites within the cell throughout division (Nebenführ et al. 2000). Brefeldin, which inhibits the supply and fusion of Golgi-derived vesicles, prevents the formation and growth of the phragmoplast and cell plate (Yasuhara and Shibaoka 2000). Thus, for the ER and Golgi, the partial localisation at the plane of division matches a role in the division process. This strongly suggests that the complete aggregation of peroxisomes at the cell plate must relate to their function(s) during division.

Our electron microscopy and immunofluorescence data show that in cells undergoing cytokinesis, a close association exists between peroxisomes and individual vesicles, and between peroxisomes and the cell plate in general. This association is similar to the close spacing of leaf peroxisomes, chloroplasts and mitochondria when these organelles are biochemically coupled in the photorespiratory pathway (Huang et al. 1983; Reumann 2002). Two possible, and not mutually exclusive functions can be suggested for these aggregated peroxisomes.

The young cell plate is initially highly fluid and must straighten and harden before the plate fuses with

the parent cell wall. In mature cell walls, hydrogen peroxide functions in secondary wall differentiation in cotton fibres (Potikha et al. 1999) and acts to strengthen the wall in several ways that reduce cell elongation (van Breusegem et al. 2001). Peroxide cross-links pectin side chains (Schopfer 1996) and catalyses the polymerisation of extensin monomers into an insoluble, cross-linked network (Cooper and Varner 1984). Consistent with this, inhibition of extensin peroxidase, the enzyme that uses peroxide to cross-link extensin monomers, also results in increased cell elongation in tomato (Brownleader et al. 2000). Although hydrogen peroxide production is not currently known in dividing cells, were the hardening of the cell plate to involve peroxide-based cross-linking of pectins or extensins, then peroxisomes adjacent to the cell plate would play two roles. First, they would scavenge any peroxide that might diffuse into the cell thereby limiting oxidative damage, and second, their preferential localisation at the expanding edge of the cell plate would ensure that this part of the cell plate would remain fluid.

It is also possible that peroxisomes adjacent to the cell plate function in the recycling of membranes, which is necessary because the surface area of the vesicles required to build the new cross wall is considerably greater than the area of new plasma membrane. Up to 75% of membrane added during *Arabidopsis* endosperm syncytial divisions is recovered (Otegui et al. 2001), and electron microscopy confirms that peroxisomes aggregate in the same area that clathrin-coated vesicles form within the developing phragmoplast membrane reticulum (Samuels et al. 1995). We suggest that the peroxisomes may metabolise excess membrane lipids not required by the cell through  $\beta$ -oxidation, and possibly the glyoxylate pathway. Typically, all plant peroxisomes are capable of the  $\beta$ -oxidation of fatty acids, and thus have been suggested to regulate the turnover of membrane lipids (Gerhardt 1986), and the recovery of lipids from membrane during senescence (Gerhardt 1992). Experiments are currently being conducted to determine whether peroxisomes aggregated at the cell plate contain enzymes such as malate synthase and isocitrate lyase, which occur only in the glyoxylate pathway.

#### Conclusions

The function(s) of actin-dependent, peroxisome aggregation adjacent to the cell plate remains unknown. Furthermore, although peroxisomes aggregate in onion cells and some other monocots, this effect does not occur in the same way in dicots such as *Arabidopsis*, perhaps reflecting differences in the biochemistry of monocot and dicot cell walls. Our development of a transient expression system that allows visualisation of leek epidermal peroxisomes with targeted GFP may prove invaluable, as it should allow the functions of peroxisome aggregation during cytokinesis to be probed more readily.

**Acknowledgements** We thank the following people for discussions and encouragement: Brian Gunning and Geoff Wasteneys (ANU), Peter Ryan and Rosemary White (CSIRO Division of Plant Industry), Robert Mullen (University of Guelph), Dick Trelease (Arizona State University) and Robyn Overall and Jan Marc (Sydney University). We also wish to thank Spencer Whitney and Grant Pearce (ANU) for assistance with the particle bombardment gun, Lynn Libous-Bailey for technical assistance, and Ellie Kable (Electron Microscopy Unit, Sydney University) and Daryl Webb (ANU) for assistance with confocal and two-photon microscopy. D.A.C. acknowledges the receipt of an ARC (Australian Research Council) Research Fellowship and Discovery Grant DP0208806, while J.D.I.H. acknowledges funding from the Farrer Centre at Charles Sturt University. Mention of a trademark, proprietary product or vendor does not constitute an endorsement by the USDA.

## References

- Boevink P, Oparka K, Santa Cruz S, Martin B, Betteridge A, Hawes C (1998) Stacks on tracks: the plant Golgi apparatus traffics on an actin/ER network. *Plant J* 15:441–447
- Brown RC, Lemmon BE (1985) Preprophasic establishment of division polarity in monoplastid mitosis of hornworts. *Protoplasma* 124:175–183
- Brown RC, Lemmon BE (1990) Monoplastidic cell division in lower land plants. *Am J Bot* 77:559–571
- Brownleader MD, Hopkins J, Mobasheri A, Dey PM, Jackson P, Trevan M (2000) Role of extensin peroxidase in tomato (*Lycopersicon esculentum* Mill.) seedling growth. *Planta* 210:668–676
- Busby CH, Gunning BES (1988) Establishment of plastid-based quadripolarity in spore mother cells of the moss *Funaria hygrometrica*. *J Cell Sci* 91:117–126
- Collings DA, Asada T, Allen NS, Shibaoka H (1998) Plasma membrane-associated actin in Bright Yellow 2 tobacco cells: evidence for interaction with microtubules. *Plant Physiol* 118:917–928
- Collings DA, Harper JDI, Marc J, Overall RL, Mullen RT (2002) Life in the fast lane: actin-based motility of plant peroxisomes. *Can J Bot* 80:430–441
- Cooper JB, Varner JE (1984) Crosslinking of soluble extensin in isolated cell walls. *Plant Physiol* 76:414–417
- Cutler SR, Ehrhardt DW, Griffiths JS, Somerville CR (2000) Random GFP::cDNA fusions enable visualization of subcellular structures in cells of *Arabidopsis* at a high frequency. *Proc Natl Acad Sci USA* 97:3718–3723
- Gerhardt B (1986) Basic metabolic function of the higher plant peroxisome. *Physiol Veg* 24:397–410
- Gerhardt B (1992) Fatty acid degradation in plants. *Prog Lipid Res* 31:417–446
- Giménez-Abián MI, Utrilla L, Cánovas JL, Giménez-Martin G, Navarrete MH, De La Torre C (1998) The positional control of mitosis and cytokinesis in higher-plant cells. *Planta* 204:37–43
- Hanzely L, Vigil EL (1975) Fine structural and cytochemical analysis of phragmosomes (microbodies) during cytokinesis in *Allium* root tip cells. *Protoplasma* 86:269–277
- Hu J, Aguirre M, Peot C, Alonso J, Ecker J, Chory J (2002) A role for peroxisomes in photomorphogenesis and development of *Arabidopsis*. *Science* 297:405–409
- Huang AHC, Trelease RN, Moore TS Jr (1983) Plant peroxisomes. Academic Press, New York
- Jedd G, Chua N-H (2002) Visualization of peroxisomes in living plant cells reveals acto-myosin-dependent cytoplasmic streaming and peroxisome budding. *Plant Cell Physiol* 43:384–392
- Kakimoto T, Shibaoka H (1988) Cytoskeletal ultrastructure of phragmoplast-nuclei complexes isolated from cultured tobacco cells. *Protoplasma [Suppl]* 2:95–103
- Liu B, Palevitz BA (1992) Organization of cortical microfilaments in dividing root cells. *Cell Motil Cytoskel* 23:252–264
- Mano S, Nakamori C, Hayashi M, Kato A, Kondo M, Nishimura M (2002) Distribution and characterization of peroxisomes in *Arabidopsis* by visualization with GFP: dynamic morphology and actin-dependent movement. *Plant Cell Physiol* 43:331–341
- Mathur J, Mathur N, Hülskamp M (2002) Simultaneous visualization of peroxisomes and cytoskeletal elements reveals actin and not microtubule-based peroxisome motility in plants. *Plant Physiol* 128:1031–1045
- McCurdy DW, Palevitz BA, Gunning BES (1991) Effect of cytochalasins on actin in dividing root tip cells of *Allium* and *Triticum*: a comparative immunocytochemical study. *Cell Motil Cytoskel* 18:107–112
- Miyagishima S, Takahara M, Kuroiwa T (2001) Novel filaments 5 nm in diameter constitute the cytosolic ring of the plastid division apparatus. *Plant Cell* 13:707–721
- Molchan TM, Valster AH, Hepler PK (2002) Actomyosin promotes cell plate alignment and late lateral expansion in *Tradescantia* stamen hair cells. *Planta* 214:683–693
- Mullen RT, Flynn CR, Trelease RN (2001) How are peroxisomes formed? The role of the endoplasmic reticulum and peroxins. *Trends Plant Sci* 6:256–261
- Nebenführ A, Frohlich JA, Staehelin LA (2000) Redistribution of Golgi stacks and other organelles during mitosis and cytokinesis in plant cells. *Plant Physiol* 124:135–151
- Ostap EM (2002) 2,3-butanedione monoxime (BDM) as a myosin inhibitor. *J Musc Res Cell Motil* 23:305–308
- Otegui M, Staehelin LA (2000) Cytokinesis in flowering plants: more than one way to divide a cell. *Curr Opin Plant Biol* 3:493–502
- Otegui MS, Mastrorarde DN, Kang B-H, Bednarek SY, Staehelin LA (2001) Three-dimensional analysis of syncytial-type cell plates during endosperm cellularization visualized by high resolution electron tomography. *Plant Cell* 13:2033–2051
- Palevitz BA, Hepler PK (1974) The control of the plane of division during stomatal differentiation in *Allium*. *Chromosoma* 46:327–341
- Parke J, Miller C, Anderton BH (1986) Higher plant myosin heavy-chain identified using a monoclonal antibody. *Eur J Cell Biol* 41:9–13
- Pickett-Heaps JD (1972) Cell division in *Klebsormidium subtilissimum* (formerly *Ulothrix subtilissima*), and its possible phylogenetic significance. *Cytobios* 6:167–183
- Porter KR, Machado RD (1960) Studies on the endoplasmic reticulum. IV. Its form and distribution during mitosis in cells of onion root tips. *J Biophys Biochem Cytol* 7:167–180
- Potikha TS, Collins CC, Johnson DI, Delmer DP, Levine A (1999) The involvement of hydrogen peroxide in the differentiation of secondary walls in cotton fibers. *Plant Physiol* 119:849–858
- Reumann S (2002) The photorespiratory pathway of leaf peroxisomes. In: Baker A, Graham IA (eds) Plant peroxisomes. Biochemistry, cell biology and biotechnology applications. Kluwer, Dordrecht, pp 141–189
- Samuels AL, Giddings TH Jr, Staehelin LA (1995) Cytokinesis in tobacco BY-2 and root tip cells: new model of cell plate formation in higher plant cells. *J Cell Biol* 130:1345–1347
- Schmit A-C (2000) Actin during mitosis and cytokinesis. In: Staiger CJ, Baluška F, Volkmann D, Barlow PW (eds) Actin: a dynamic framework for multiple plant cell functions. Kluwer, Dordrecht, pp 437–456
- Schopfer P (1996) Hydrogen peroxide-mediated cell-wall stiffening in vitro in maize coleoptiles. *Planta* 199:43–49
- Valster AH, Hepler PK (1997) Caffeine inhibition of cytokinesis: effect on the phragmoplast cytoskeleton in living *Tradescantia* stamen hair cells. *Protoplasma* 196:155–166
- van Breusegem F, Vranová E, Dat JF, Inzé D (2001) The role of reactive oxygen species in plant signal transduction. *Plant Sci* 161:405–414
- Vaughn KC, Hoffman JC, Hahn MG, Staehelin LA (1996) The herbicide dichlobenil disrupts cell plate formation: immunogold characterization. *Protoplasma* 194:117–132
- Warren G, Wickner W (1996) Organelle inheritance. *Cell* 84:395–400

- Yamamoto K, Hamada S, Kashiya T (1999) Myosins from plants. *Cell Mol Life Sci* 56:227–232
- Yasuhara H, Shibaoka H (2000) Inhibition of cell-plate formation by brefeldin A inhibited the depolymerization of microtubules in the central region of the phragmoplast. *Plant Cell Physiol* 41:300–310
- Zhang D, Wadsworth P, Hepler PK (1993) Dynamics of microfilaments are similar, but distinct from microtubules during cytokinesis in living, dividing plant cells. *Cell Motil Cytoskel* 24:151–155